



# Bipyridyl/cbazolate silver(I) and gold(I) N-heterocyclic carbene complexes: A systematic study of geometric constraints and electronic properties

Sirsendu Das Adhikary<sup>1</sup> | Ambarish Mondal<sup>2</sup> | Hemanta K. Kisan<sup>2</sup> |  
Christopher W. Bielawski<sup>3,4,5</sup> | Joydev Dinda<sup>2</sup>

<sup>1</sup>School of Applied Science, Haldia Institute of Technology, Haldia, 721657, West Bengal, India

<sup>2</sup>Department of Chemistry, Utkal University, Vani Bihar, Bhubaneswar, 751004, Odisha, India

<sup>3</sup>Center for Multidimensional Carbon Materials (CMCM), Institute for Basic Science (IBS), Ulsan, 44919, Republic of Korea

<sup>4</sup>Department of Chemistry, Ulsan National Institute of Science and Technology (UNIST), Ulsan, 44919, Republic of Korea

<sup>5</sup>Department of Energy Engineering, Ulsan National Institute of Science and technology (UNIST), Ulsan, 44919, Republic of Korea

## Correspondence

Joydev Dinda, Department of Chemistry, Utkal University, Vani Bihar, Bhubaneswar 751004, Odisha, India.  
Email: dindajoy@yahoo.com

## Funding information

Ministry of Education and the National Research Foundation, Grant/Award Numbers: IBS-R019-D1, IBS-R019; Science and Engineering Research Board, Grant/Award Number: EMR/2016/007022

A series of silver(I) and gold(I) carbene complexes of the type  $[M(L)(2,2'-bipyridine)][PF_6]$  ( $L = 1\text{-benzyl-3-(2-pyridylmethyl)benzimidazolylidene}$ ;  $M = \text{Ag (1)}$ ;  $M = \text{Au (3)}$ ) and  $[M(L)(\text{carbazole})]$  ( $M = \text{Ag (2)}$ ;  $M = \text{Au (4)}$ ) were synthesized and analyzed using a range of spectroscopic and crystallographic techniques. Inspection of the solid-state structures of **1**, **2** and **4** revealed a number of intermolecular noncovalent interactions. In the solid-state structure adopted by **1**,  $\pi-\pi$  and Ag–Ag interactions directed the complexes to orient in a head-to-tail fashion. The photophysical properties were found to be influenced by the ancillary ligands in solution as well as in the solid-state. Calculations were performed to support the aforementioned structural and optoelectronic assignments.

## KEY WORDS

N-heterocyclic carbene, gold(I)-NHC, silver(I)-NHC, photoluminescent, carbazole

## 1 | INTRODUCTION

In 1991, Arduengo and co-workers successfully isolated 1,3-di(adamantyl)imidazol-2-ylidene as the first stable N-heterocyclic carbene (NHC).<sup>[1]</sup> Since this hallmark event, it has been determined that significant electron density resides on the carbene nuclei of NHCs, which are typically nucleophilic and thus can be distinguished from

their electrophilic carbene analogues.<sup>[2]</sup> NHCs are also strong  $\sigma$ -electron donors, similar to phosphines, and offer a number of advantages when compared to other ligands due, in part, to a high thermal stability and unique structural parameters.<sup>[3]</sup> Moreover, NHCs have been shown to bind to a broad range of transition metals in high as well as low oxidation states.<sup>[4]</sup> Particular interest in Ag(I) and Au(I) supported by NHCs has grown over the past several

decades because such complexes hold potential for use in a range of medicinal,<sup>[5]</sup> electronic<sup>[6]</sup> and materials applications.<sup>[7–9]</sup> Due to such versatility and accessibility, NHC ligands represent an attractive scaffold for constructing new complexes.<sup>[10]</sup>

2,2'-Bipyridine (bpy) and its derivatives have also been the subject of numerous studies in coordination chemistry due to their abilities to form chelates as well as their useful photophysical properties.<sup>[11–13]</sup> Likewise, carbazole (cbz), a strong σ-donor commonly used in hole-transporting applications, has also been extensively studied as a ligand.<sup>[14]</sup> The integration of bpy or cbz was hypothesized to influence the fundamental electronic and photophysical properties displayed by metal complexes supported by NHCs. For example, bpy was expected to enhance π-backbonding interactions and thus electronic delocalization, whereas cbz was expected to place more electron density on the coordinated metal.<sup>[14]</sup> Finally, since there are relatively few known metals that are supported by NHCs and bpy<sup>[12,13]</sup> or cbz<sup>[14]</sup> ligands, we envisioned enriching our understanding of such types of complexes through the synthesis of new derivatives.

## 2 | RESULTS AND DISCUSSION

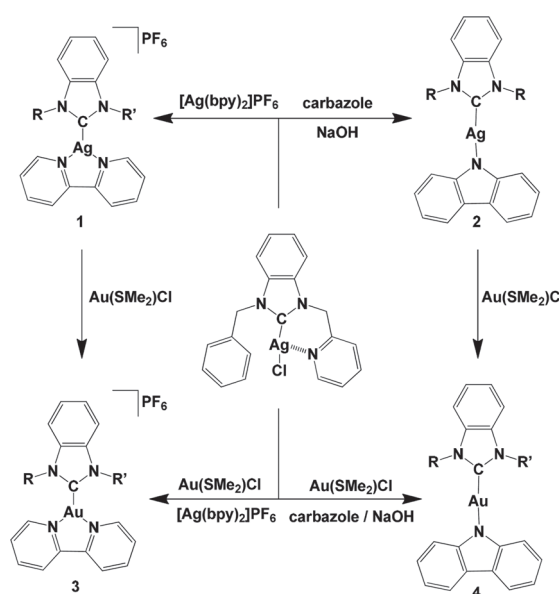
The synthetic procedures used to prepare the target complexes are summarized in Scheme 1.<sup>[15]</sup> The requisite NHC precursor, 1-benzyl-3-(2-pyridylmethyl)benzimidazolium chloride, was prepared from 1-benzylbenzimidazole and picolylchloride hydrochloride in ethanol under basic conditions.<sup>[16]</sup> Treatment of the salt with

$\text{Ag}_2\text{O}$  in dichloromethane at room temperature afforded  $[\text{Ag}(1\text{-benzyl-3-(2-pyridylmethyl)benzimidazolylidene})\text{Cl}]$  ( $[\text{Ag}(\text{L})\text{Cl}]$ ).<sup>[17]</sup> The  $[\text{Ag}(\text{L})(\text{bpy})]\text{PF}_6$  complex **1** was synthesized by treating  $[\text{Ag}(\text{L})\text{Cl}]$  with an equimolar quantity of  $[\text{Ag}(\text{bpy})_2]\text{PF}_6$  in acetonitrile at room temperature. The  $[\text{Au}(\text{L})(\text{bpy})]\text{PF}_6$  complex **3** was obtained by transmetallating **1** with  $\text{Au}(\text{SMe}_2)\text{Cl}$ .<sup>[18]</sup> Alternatively, the same complex was obtained upon introducing  $[\text{Au}(\text{L})\text{Cl}]$  to  $[\text{Ag}(\text{bpy})_2]\text{PF}_6$ .

The formation of **1** and **3** were independently confirmed in part using multi-nuclear NMR spectroscopy and other analytical techniques. The presence of the carbene nuclei was supported by the appearances of  $^{13}\text{C}$  NMR signals at 163.9 and 166.7 ppm for **1** and **3**, respectively. Further support for the structural assignment of **1** was obtained from an X-ray diffraction analysis and will be described in more detail below. As X-ray-quality single crystals of **3** remained elusive, an optimized molecular structure was calculated and will also be discussed below.

Complex **2** was synthesized by treating  $[\text{Ag}(\text{L})\text{Cl}]$  with cbz in a basic mixture of dichloromethane and water. After isolation and evaporation of the organic solvent, the residual solid was recrystallized from dichloromethane and diethyl ether to afford **2**. Transmetallation of **2** with  $\text{Au}(\text{SMe}_2)\text{Cl}$  afforded **4**. Likewise, treatment of  $[\text{Au}(\text{L})\text{Cl}]$  under basic conditions afforded the same complex. Multi-nuclear NMR spectroscopy, X-ray crystallography and other analytical techniques were used to elucidate the structures and to assess the purities of **2** and **4**. Collectively, complexes **1–4** were prepared in good yields, isolated as colorless to light yellow solids and were found to be stable under ambient conditions.

In order to unambiguously confirm the structural assignment of **1**, single crystals were obtained by slowly diffusing diethyl ether into a saturated acetonitrile solution of **1** at room temperature. The solid-state structure adopted by **1** is depicted in Figure 1; selected crystallographic parameters and bond parameters are listed in Tables 1 and 2, respectively. Complex **1** crystallized in the triclinic space group *p*-1. The Ag–carbene bond distance,  $\text{Ag}(1)\text{–C}(1)$ , was measured to be 2.089(2) Å, consistent with that reported for a bis(benzimidazolylidene) silver(I) hexafluorophosphate (2.086(3) Å)<sup>[17]</sup> and less than the sum of the covalent radii of the constituent carbon and silver atoms (2.111 Å). The  $\text{Ag}(1)\text{–N}(4)$  and  $\text{Ag}(1)\text{–N}(5)$  bond distances were measured to be 2.337(2) and 2.272(2) Å, respectively, and the  $\text{N}(1)\text{–C}(1)\text{–N}(2)$  bond angle was measured to be 105.9(2)°; these values were comparable to analogues reported in the literature.<sup>[19]</sup> The  $\text{N}(4)\text{–Ag}(1)\text{–N}(5)$ ,  $\text{N}(4)\text{–Ag}(1)\text{–C}(1)$  and  $\text{N}(5)\text{–Ag}(1)\text{–C}(1)$  angles were measured at 71.68(8)°,



**SCHEME 1** Syntheses of complexes **1–4** ( $\text{R} = \text{benzyl}$ ;  $\text{R}' = \text{2-picolyl}$ )

**FIGURE 1** Single-crystal X-ray structure of **1** (right) and optimized geometry of **3** (left). Hydrogen atoms and counter anions have been removed for clarity

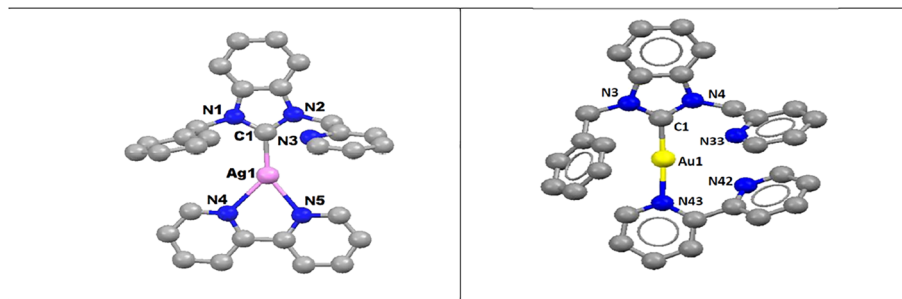


**TABLE 1** Summary of crystal X-ray structure parameters

	<b>1</b>	<b>2</b>	<b>4</b>
Empirical formula	C <sub>30</sub> H <sub>25</sub> AgN <sub>5</sub> F <sub>6</sub> P	C <sub>32</sub> H <sub>25</sub> AgN <sub>4</sub>	C <sub>32</sub> H <sub>25</sub> AuN <sub>4</sub>
Formula weight	708.39	573.43	662.53
Temperature	295	293(2)	293(2)
Crystal system	Triclinic	Monoclinic	Monoclinic
Unit cell dimensions			
<i>a</i> (Å)	9.2368(2)	24.744(14)	26.942(7)
<i>b</i> (Å)	13.1310(3)	10.057(5)	9.772(2)
<i>c</i> (Å)	13.3482(4)	21.621(10)	21.448(5)
$\alpha$ (°)	115.9631(9)	90.00	90.00
$\beta$ (°)	94.5730(8)	97.404(18)	109.788(9)
$\gamma$ (°)	96.8450(13)	90.00	90.00
Volume	1429.35(6)	5336(5)	5313(2)
<i>Z</i>	2	8	8
Calcd density (Mg m <sup>-3</sup> )	1.646	1.428	1.656
Absorption coefficient	0.831	0.783	5.565
$\theta$ range (°)	2.85–30.00	1.66–23.51	1.61–25.00
No. of reflns collected	8215	3912	3413
No. of ind. reflns	6209	19669	4679
Goodness-of-fit on <i>F</i> <sup>2</sup>	1.051	1.122	1.013
Final <i>R</i> indices [ <i>I</i> > 2σ( <i>I</i> )]	R1 = 0.0459 wR2 = 0.1228	R1 = 0.0678 wR2 = 0.1704	R1 = 0.0833 wR2 = 0.2126
<i>R</i> indices (all data)	R1 = 0.0673 wR2 = 0.1325	R1 = 0.0865 wR2 = 0.1868	R1 = 0.1043 wR2 = 0.2413

**TABLE 2** Selected bond lengths and bond angles measured in the solid-state structures of **1** and **3** along with calculated values

<b>Bond lengths (Å)</b>			<b>Bond angles (°)</b>			
<b>1</b>	<b>3</b>		<b>1</b>	<b>3</b>		
	Expt	Calcd		Expt	Calcd	
Ag(1)–C(1)	2.089(2)	2.1074	2.0101	N(1)–C(1)–N(2)	105.9(2)	105.81
Ag(1)–N(4)	2.337(2)	2.3223	2.1185	C(1)–Ag(1)–N(4)	139.14(9)	133.06
Ag(1)–N(5)	2.272(2)	2.4132	—	C(1)–Ag(1)–N(5)	148.47(9)	156.33
C(1)–N(1)	1.351(3)	1.3614	1.3601	N(4)–Ag(1)–N(5)	71.68(8)	70.21
C(1)–N(2)	1.347(3)	1.3582	1.3575			—

139.14(9) $^{\circ}$  and 148.47(9) $^{\circ}$ , respectively. The smallest angle reflects chelation of the bpy ligand with the Ag center. The imidazole ring and bpy were observed to be nearly coplanar with a dihedral angle of 6.22 $^{\circ}$ . As shown in Figure 2, the crystal packing diagram revealed that the complexes arranged in a head-to-tail fashion due to the formation of  $\pi$ - $\pi$  and Ag–Ag interactions.<sup>[20]</sup> The Ag–Ag distance (3.130 Å) was measured to be shorter than the sum of the constituent van der Waals radii (4.26 Å)<sup>[21a]</sup> yet longer than a typical Ag–Ag covalent bond (2.611 Å).<sup>[21b]</sup>

The calculated structure of **3** revealed that the geometry about the Au center was nearly linear (C1-Au1-N43 = 174.34 $^{\circ}$ ) where one nitrogen atom of the bpy ligand was coordinated to Au and the other remained as a free base. The Au–C<sub>carbene</sub> distance was measured (2.0101 Å) to be similar to analogous distances reported for other Au–NHC complexes.<sup>[15,19]</sup> All other bond parameters calculated for **3** were similar to the experimental values determined for **1**. For example, the N3–C1–N4 angle (106.64 $^{\circ}$ ) is only slightly larger than the corresponding experimentally determined value for **1** (105.9(2) $^{\circ}$ ). Collectively, these data support the veracity of the computational method employed.

Single crystals suitable for X-ray analysis were grown by slowly diffusing diethyl ether into a saturated acetonitrile solution of **2** at room temperature. The corresponding structure of the complex is depicted in Figure 3. Selected crystallographic parameters and bond parameters are listed in Tables 1 and 3, respectively.

Complex **2** crystallized in the monoclinic space group C2/c. The geometry of the Ag(I) center was found to be linear as indicated by the C(1)–Ag(1)–N(4) angle of 174.79(19) $^{\circ}$ . The imidazole and carbazolate rings were

**TABLE 3** Selected bond lengths (Å) and bond angles ( $^{\circ}$ ) measured in the solid-state structures of **2** and **4** along with calculated values

	Ag-cbz (2)		Au-cbz (4)	
	Expt	Calcd	Expt	Calcd
M(1)–C(1)	2.073(6)	2.084	1.979(14)	2.011
M(1)–N(4)	2.072(5)	2.063	1.997(11)	2.026
C(1)–N(1)	1.370(8)	1.364	1.347(18)	1.362
C(1)–N(2)	1.341(9)	1.358	1.419(19)	1.366
N(1)–C(1)–N(2)	107.0(5)	105.83	106.8(12)	106.07
C(1)–M(1)–N(4)	174.79(19)	172.23	177.8(5)	174.25
C(21)–N(4)–C(32)	105.9(5)	106.38	105.3(11)	106.78

nearly coplanar with a dihedral angle of 9.0 $^{\circ}$ . The Ag–C<sub>carbene</sub> distance (2.073(6) Å) is similar to that of other reported Ag(I)–NHC structures<sup>[19]</sup> and less than the sum of the covalent radii of the constituent carbon and silver atoms (2.111 Å). The C(1)–N(1) and C(1)–N(2) bond lengths were measured to be 1.370(8) and 1.341(9) Å, respectively. The Ag–N<sub>cbz</sub> bond distance (Ag(1)–N(4) = 2.072(5) Å) was measured to be shorter than the Ag(1)–N<sub>bpy</sub> distance found in complex **1**, which may reflect a relatively strong bonding interaction between the Ag(I) center and the cbz ligand.

Single crystals suitable for X-ray analysis were grown by slowly diffusing diethyl ether into a saturated acetonitrile solution of **4** at room temperature. The structure of **4** is depicted in Figure 3. Selected crystallographic parameters and bond parameters are listed in Tables 1 and 3,

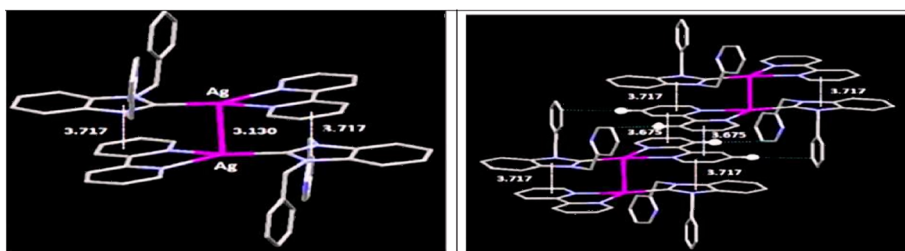


**FIGURE 2** Packing view of **1** showing C–H– $\pi$ ,  $\pi$ – $\pi$  and Ag–Ag interactions

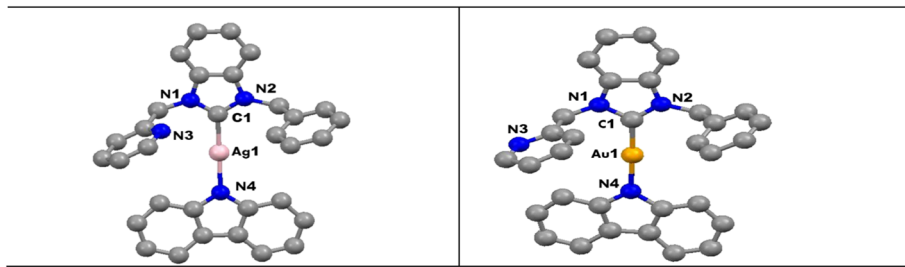


**FIGURE 3** ORTEP view (50% probability) of **2** (left) and single-crystal X-ray structure of **4** (right). Hydrogen atoms have been removed for clarity

respectively. The Au–C<sub>carbene</sub> (1.979(14) Å) and Au–N<sub>cbz</sub> (1.997(11) Å) distances were measured to be shorter than the analogous values measured for **2** and comparable to values reported in the literature.<sup>[14]</sup> The Au–C<sub>carbene</sub> distance is less than the sum of the covalent radii of the constituent Au (1.66 Å) and C (1.70 Å) atoms.<sup>[19]</sup> The C(1)–Au(1)–N(4) angle was measured to be 177.8(5)°.

Comparing the Ag–C<sub>carbene</sub> or Au–C<sub>carbene</sub> bond distances measured in **1** versus **3** (2.086(3) versus 2.073(6) Å, respectively) or **2** versus **4** (1.992(14) versus 1.979(14) Å, respectively) revealed that the carbazole unit had a limited effect on the M–C<sub>carbene</sub> bond length. For example, the Ag–C<sub>carbene</sub> bond distance (2.073(6) Å) measured in the solid-state structure of **2** was only slightly shorter than the analogous distance measured in [Ag(L)<sub>2</sub>][PF<sub>6</sub>] (2.086(3) Å).<sup>[17]</sup> Similarly, the Au–C<sub>carbene</sub> bond distance (1.979(14) Å) measured in the solid-state structure of **4** was only slightly shorter than the analogous distance measured in [Au(L)<sub>2</sub>][PF<sub>6</sub>] (1.992(14) Å).<sup>[15]</sup> Likewise, the C–N bond distances found in the solid-state

structures of **2** and **4** were nearly identical to those measured in [M(L)<sub>2</sub>][PF<sub>6</sub>] complexes (M = Ag or Au).

Absorption and luminescence data were recorded for complexes **1**–**4** in CH<sub>3</sub>CN or in the solid-state. As shown in Figures 4–6 and summarized in Table 4, all of the complexes exhibited weak absorption bands in the range 355–370 nm, which were assigned to metal-to-ligand charge transfer (MLCT) processes.<sup>[12]</sup> The complexes exhibited absorption maxima between 240 and 280 nm, which were assigned to intra-ligand (IL)  $\delta$ – $\delta^*$  transitions. The highest energy transitions displayed by **2** and **4** were blue-shifted and centered at *ca* 230 nm. Complex **4** also displayed two intense red-shifted bands at 306 and 317 nm, which may be due to extended conjugation. All of the complexes displayed high-energy emissions between 400 and 440 nm upon excitation at 280–295 nm.

In the solid-state, the emission bands displayed by complexes **1** and **2** appeared at 525–545 nm whereas those exhibited by **3** and **4** were measured at 525–570 nm (as presented in Table 4). While the NHC ligand (L) and

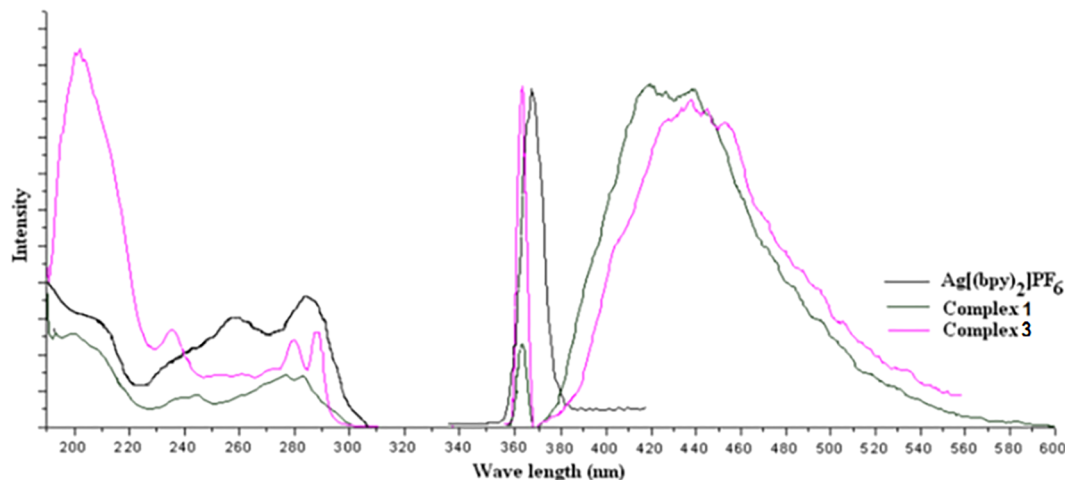


**FIGURE 4** Emission (right) and excitation (left) spectra recorded for various complexes (indicated) in acetonitrile at room temperature

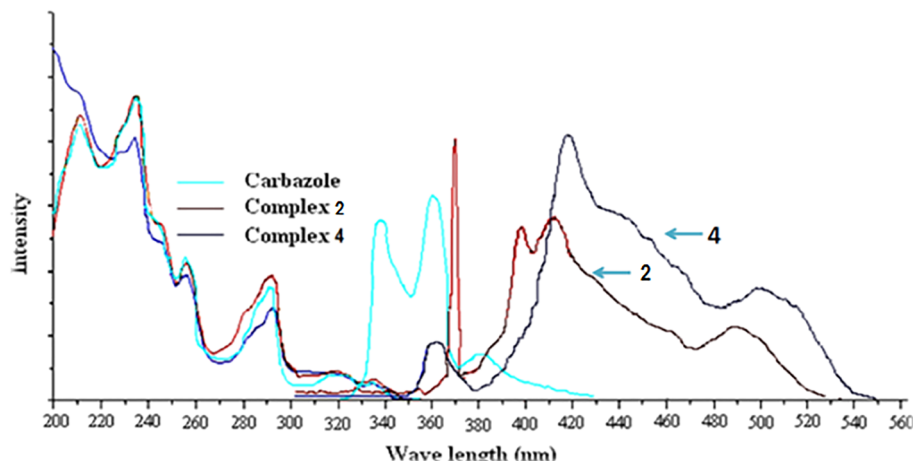


**FIGURE 5** Emission (right) and excitation (left) spectra recorded for **2** and **4** in acetonitrile at room temperature

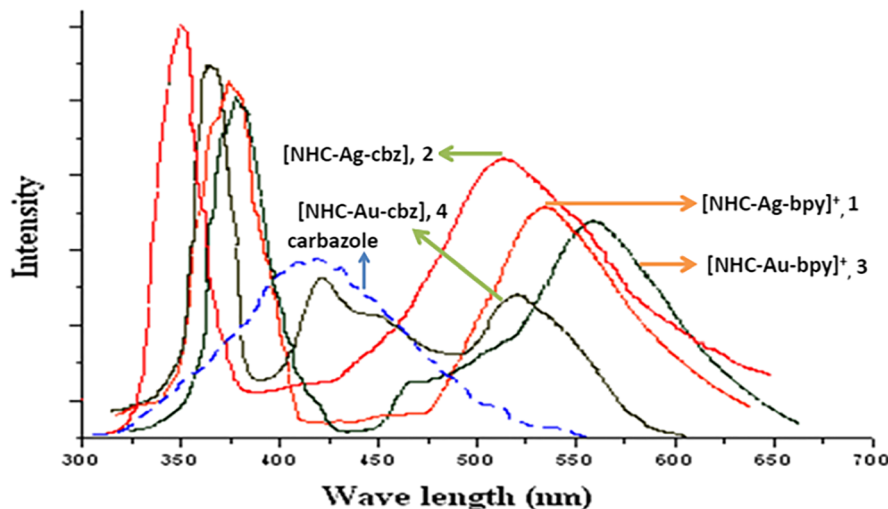


**FIGURE 6** Emission spectra of various complexes and free carbazole (indicated) as measured in the solid-state at room temperature

**TABLE 4** Photoluminescence data recorded for **1–4**

Complex	$\lambda_{\text{ex}}^{\text{a,b}}$	$\lambda_{\text{em}}^{\text{a,b}}$	$\lambda_{\text{em}}^{\text{a,c}}$
[NHC-Ag-bpy] <sup>+</sup> , <b>1</b>	280	430	540
[NHC-Au-bpy] <sup>+</sup> , <b>3</b>	280	440	567
[NHC-Ag-cbz], <b>2</b>	285	415	515
[NHC-Au-cbz], <b>4</b>	285	422	523

<sup>a</sup>Data were recorded at room temperature and the values reported are in nanometers (nm).

<sup>b</sup>Data were recorded in solution.

<sup>c</sup>Data were recorded in the solid-state.

NHC–Ag(I)–Cl are non-luminescent,  $d^{10}$  configurations of silver or gold ions can be expected to combine with the  $\pi^*$  orbitals of the ligands to produce MLCT and/or IL transitions, which result in luminescence.<sup>[12]</sup> In the solid-state, complex **1** exhibits luminescence at 545 nm and **2** at 570 nm; similarly, complex **3** exhibits luminescence at 525 nm and **4** at 527 nm. In other words, solid-state emission is red-shifted when compared to that measured in solution. The origin of the emissions observed at 532 and 575 nm for **1** and **2** may be due to metal-perturbed IL transitions, whereas the high-energy emission at 325–430 nm may stem from IL  $\pi$ – $\pi^*$  transitions. Regardless, the ancillary ligands (bpy versus cbz) appeared to play a prominent role in determining the intrinsic photophysical properties displayed by the complexes.<sup>[14]</sup>

In order to further support the structural assignments described above, complexes **1–4** were examined using density functional theory (DFT) at the B3LYP level (see Figures 7–9 and 4–6). A natural bond orbital (NBO) analysis was also conducted to elucidate the electronic structures of the complexes.<sup>[22]</sup> As summarized in Tables 2 and 3, agreement between the calculated structures and the solid-state structures was excellent. The HOMOs calculated for **1** and **3** are localized primarily on the metal

centers and the NHCs. For comparison, the LUMOs of the same complexes were calculated to localize on the bpy units. As such, MLCT from the metal centers to the bpy ligands or ILCT from the NHC to the bpy ligands can be expected.<sup>[12]</sup>

For comparison, the HOMOs of **2** and **4** were calculated to localize primarily on cbz, whereas the NHC dominated the LUMOs. As such, ILCT should proceed from the cbz unit to the NHC ligand. The presence of a ligand-to-ligand charge transfer band in the visible spectrum may be expected on the basis of the calculated electronic structure. Indeed, the color of the complex was found to be off-white to light yellow and the only absorption found in the UV–visible spectra stemmed primarily from transitions that were observed in the UV region (Figures 4 and 5).

The chemical reactivities of the complexes were compared on the basis of chemical hardness ( $\eta$ ) values, as postulated by Parr and Pearson, who described a relationship between  $\eta$  and the energy gap ( $\Delta E$ ) of the frontier molecular orbitals ( $\eta = (E_{\text{LUMO}} - E_{\text{HOMO}})/2$ ).<sup>[23]</sup> From the data in Table 5, one may conclude that the Au complex **3** is more reactive than the Ag complex **1**, presumably due to an open coordinate site in the former. NBO analyses confirmed that the natural charges on the Ag atoms in **1** and **2** ranged between +0.511 and +0.456, respectively (see also the Wiberg bond indices (WBIs) listed in Table 6). However, the charges on the Au atoms in **3** and **4** were calculated to range between +0.334 and +0.322, respectively. The relative contributions may stem from the NHC and the ancillary ligands. Indeed, the former was calculated to significantly contribute (99%) to the frontier molecular orbitals of the requisite complexes. As expected, the Au–C<sub>carbene</sub> bonds were found to be shorter than Ag–C<sub>carbene</sub> bonds and were consistent with values reported in the literature.<sup>[24]</sup>

**FIGURE 7** Frontier molecular orbitals calculated for **1** (left) and **3** (right)

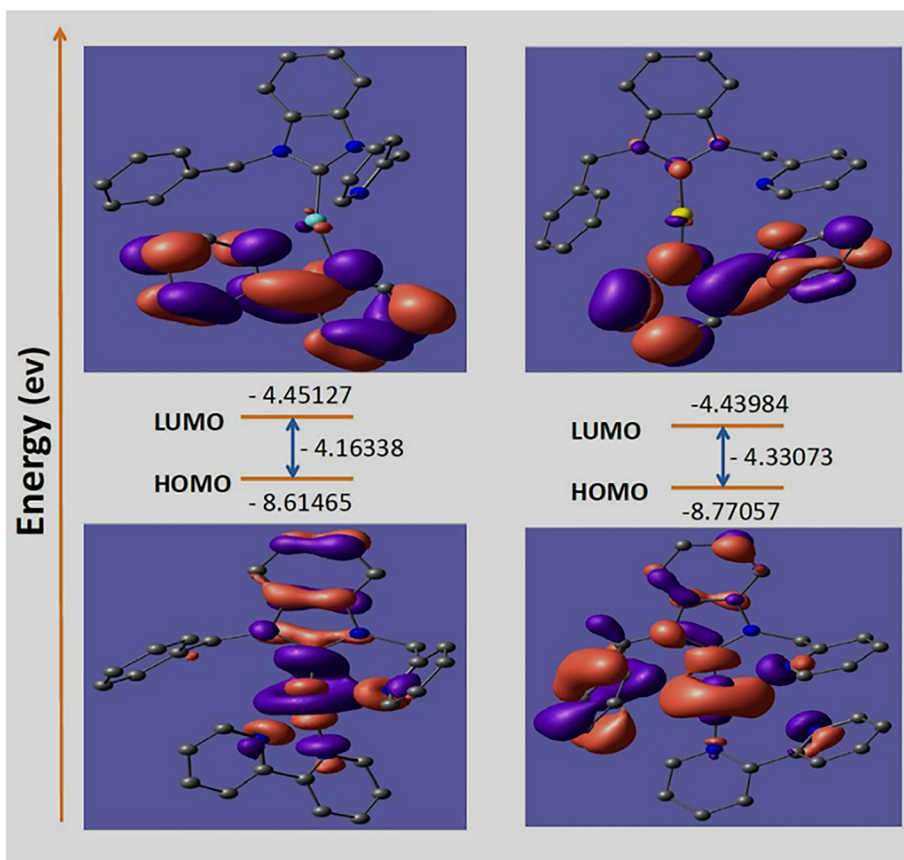
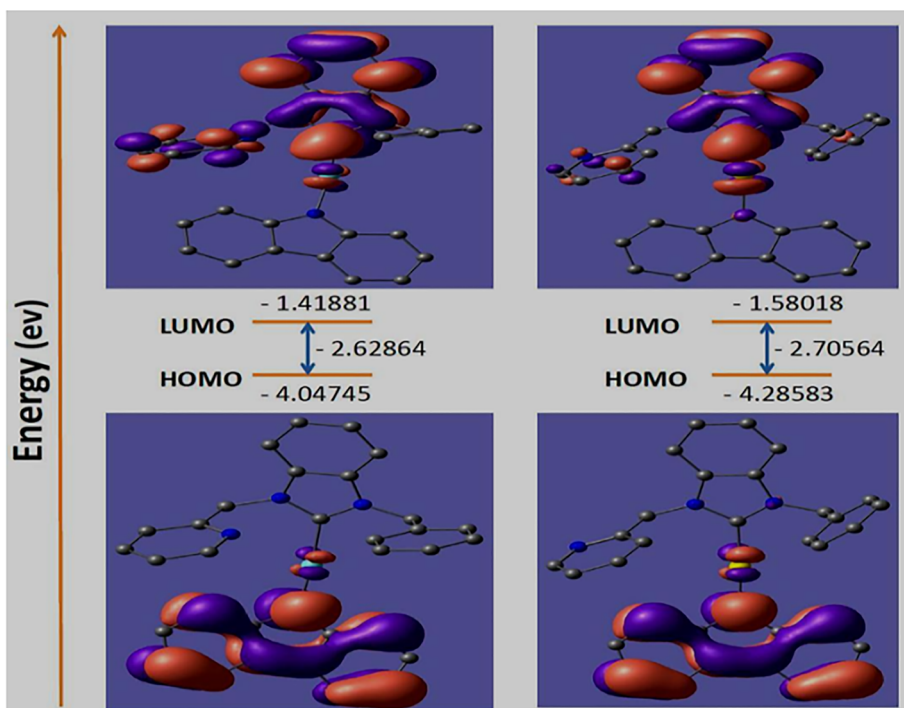


**FIGURE 8** Frontier molecular orbitals calculated for **2** (left) and **4** (right)



The analysis of the molecular orbitals of complex **1** in the dimeric form provided support for the formation of intermolecular Ag...Ag interactions. The overlapping of  $d_{z^2}$  orbitals on the silver centers revealed a strong

bonding interaction, although an antibonding interaction was also observed (Figure 9). Plots of the molecular orbitals for the dimeric form of **1** revealed that the Ag atoms constitute a major contribution to a HOMO with a

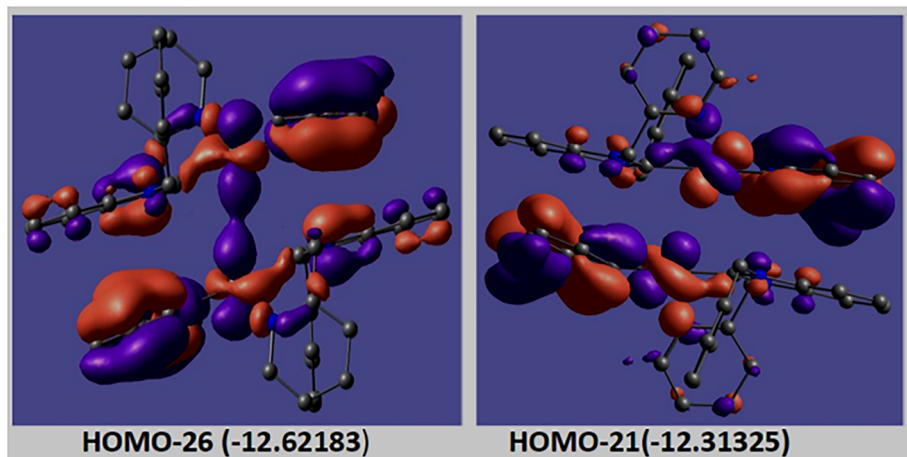


**FIGURE 9** Depiction of the calculated Ag–Ag bonding (HOMO-26) and antibonding (HOMO-21) orbitals in **1**

**TABLE 5** Chemical hardness ( $\eta$ ) values calculated for **1–4**

Complex	Chemical hardness ( $\eta$ )
<b>1</b>	2.08169
<b>2</b>	2.16537
<b>3</b>	1.31432
<b>4</b>	1.35282

**TABLE 6** Calculated WBI values

Compound	WBI (bond order)
<b>1</b>	[Ag(1)–C(1)]: 0.5189
	[Ag(1)–N(4)]: 0.1433
	[Ag(1)–N(5)]: 0.1837
<b>2</b>	[Ag(1)–C(1)]: 0.4937
	[Ag(1)–N(4)]: 0.3932
<b>3</b>	[Au(1)–C(1)]: 0.7042
	[Au(1)–N(4)]: 0.3297
	[Au(1)–N(5)]: 0.0577
<b>4</b>	[Au(1)–C(1)]: 0.6693
	[Au(1)–N(4)]: 0.4750

moderate involvement of the NHC and bpy fragments. The contributions of the Ag atoms and the NHC components in the other calculated molecular orbitals were found to be similar, even though a contribution that originated from the bpy ligand was identified.

The strength of the Ag–Ag interactions was assessed using DFT and the bond order was calculated using three methods: WBIs, natural atomic orbital (NAO) bond order and molecular orbital (MO) bond order. The corresponding bond orders were calculated as follows: WBI, 0.1201; NAO, 0.3112; MO, 0.2660 (as presented in Table 7). The positive value of the bond order is consistent with the existence of a net bonding interaction in the

**TABLE 7** Calculated bond order for dinuclear complex

Dinuclear complex	Bond order
WBI	0.120
NAO	0.311
MO	0.266

Ag–Ag couple. In the case of the NAO method, the Ag–Ag bond strength was found to be approximately one-fourth that of a typical covalent bond. For comparison, the bond strength was found to be one-third that of a typical covalent bond using the MO bond order method.

### 3 | CONCLUSIONS

The synthesis, structures and photophysical properties of a series of Ag(I) and Au(I) complexes supported by 1-benzyl-3-(2-pyridylmethyl)benzimidazolylidene and either bpy- or cbz-based ligands were described. X-ray crystallography revealed that  $\pi$ - $\pi$  and Ag–Ag interactions governed the structures of the aforementioned complexes in the solid-state. Such observations are expected to enrich to crystal engineering design parameters used to create higher order structures. The electronic and optical properties of the complexes were also examined and found to depend on the ancillary ligands as well as on the constituent metals. Many of the aforementioned assignments were corroborated by a series of DFT calculations which were in good agreement with the experimental data. Collectively, integrating bpy or cbz ligands into NHC-supported complexes is expected to facilitate refinement of

metal complexes used in contemporary electronics applications.

## 4 | EXPERIMENTAL

### 4.1 | General procedures

Reagents were purchased from Sigma-Aldrich and used without further purification. All manipulations were carried out under ambient atmosphere unless otherwise stated. All solvents were distilled over appropriate drying agents. NMR spectra were recorded using Bruker 400 spectrometers at 25°C with tetramethylsilane as an internal standard. Absorption and emission spectra were recorded using Shimadzu UV-1601 and PerkinElmer LS 55 spectrometers, respectively. The complexes [Ag(L)Cl] and [Au(L)Cl] reported earlier were prepared as previously described.<sup>[17]</sup>

### 4.2 | Synthesis of 1-benzyl-3-(2-pyridylmethyl)-1H-benzimidazolium chloride

The synthesis of this salt has been previously reported.<sup>[15]</sup> An alternative procedure is as follows. 1-Benzylbenzimidazole (500 mg, 2.4 mmol), 2-picolylichloride hydrochloride (316 mg, 1.93 mmol) and NaHCO<sub>3</sub> (211 mg, 2.51 mmol) were refluxed in EtOH for 28 h. The residual solvent was then removed, and the residual gummy mass was triturated with dichloromethane. Recrystallization from dichloromethane and Et<sub>2</sub>O afforded the desired compound as a colorless solid (564 mg, 1.68 mmol, 70% yield). <sup>1</sup>H NMR (400 MHz, CD<sub>3</sub>CN, δ, ppm): 9.38 (s, NCHN, 1H), 8.48 (d, 1H, J = 4.8 Hz, pyridine-H), 7.82 (d, 2H, J = 8.0 Hz), 7.73 (m, 1H), 7.53–7.44 (m, 5H), 7.38–7.32 (m, 3H), 7.23–7.22 (m, 1H), 5.79 (s, 2H, CH<sub>2</sub>), 5.63 (s, 2H, CH<sub>2</sub>). <sup>13</sup>C NMR (100 MHz, DMSO-d<sub>6</sub>, δ, ppm): 153.28, 149.2, 143.6, 137.3, 132.1, 131.5, 130.7, 129.0, 128.8, 127.9, 127.8, 126.6, 123.5, 123.4, 114.2, 112.9, 52.1, 51.2. Anal. Calcd for C<sub>20</sub>H<sub>18</sub>N<sub>3</sub>Cl (%): C, 71.54; H, 5.37; N, 14.31; found (%): C, 71.38; H, 5.33; N, 14.20.

### 4.3 | Synthesis of complex 1

After adding the complex [Ag(L)Cl] (60 mg, 0.14 mmol) to 10 ml of dichloromethane, an acetonitrile solution of [Ag(bpy)<sub>2</sub>]PF<sub>6</sub> (77 mg, 0.14 mmol) was introduced dropwise at room temperature; the formation of a white precipitate (AgCl) was immediately observed. After 2 h,

the precipitate was removed via filtration, and then the solvent was evaporated. The residual solid was recrystallized from CH<sub>3</sub>CN-Et<sub>2</sub>O to afford the desired complex as a colorless solid (69 mg, 0.098 mmol, 70% yield).

<sup>1</sup>H NMR (DMSO-d<sub>6</sub>, 300 MHz, 25°C, δ, ppm): 8.62 (d, J = 7.6 Hz, bpy, 4H), 8.58 (m, bpy, 4H), 8.57 (d, J = 7.6 Hz, py, 2H), 7.68 (m, py, 2H), 7.45 (d, J = 7.6 Hz, bzimi, 2H), 7.43–7.41 (m, bzimi, 2H), 7.37 (d, J = 6.8 Hz, bzyl, 2H), 7.32–7.26 (m, bzyl, 3H), 5.87 (s, CH<sub>2</sub>, 2H), 5.83 (s, CH<sub>2</sub>, 2H). <sup>13</sup>C NMR (DMSO-d<sub>6</sub>, 100.5 MHz, 25°C, δ, ppm): 163.9, 154.3, 151.5, 149.3, 149.1, 148.7, 148.5, 148.3, 137.5, 137.4, 127.3, 126.2, 123.3, 122.1, 120.78, 117.8, 117.5, 116.1, 115.7, 114.3, 113.1, 112.5, 46.4, 45.6. Anal. Calcd for C<sub>30</sub>H<sub>25</sub>N<sub>5</sub>AgPF<sub>6</sub> (%): C, 50.85; H, 3.53; N, 9.89; found (%): C, 50.68; H, 3.49; N, 9.80.

### 4.4 | Synthesis of complex 2

A dichloromethane (20 ml) solution of complex [Ag(L)Cl] (141 mg, 0.33 mmol) was treated with carbazole (55 mg, 0.33 mmol) followed by NaOH (0.5 N, 2 ml) and Bu<sub>4</sub>NCl (0.07 mmol). The resulting mixture was stirred for 2 days. Afterward, 50 ml of deionized water was added, and the resulting mixture was stirred for an additional hour. The organic component was extracted into dichloromethane and then concentrated to give a yellow residue.<sup>[14]</sup> Recrystallization from CH<sub>3</sub>CN-Et<sub>2</sub>O afforded the desired complex as a white solid (160.5 mg, 0.28 mmol, 85% yield). <sup>1</sup>H NMR (DMSO-d<sub>6</sub>, 300 MHz, 25°C, δ, ppm): 8.54 (d, J = 7.6 Hz, py, 2H), 8.01 (d, J = 4.8 Hz, cbz, 2H), 7.78 (m, cbz, 4H), 7.68 (m, py, 2H), 7.48 (d, J = 5.8 Hz, cbz, 2H), 7.45 (d, J = 7.6 Hz, bzimi, 2H), 7.42–7.38 (m, bzimi, 2H), 7.36 (d, J = 6.8 Hz, bzyl, 2H), 7.28–7.26 (m, bzyl, 3H), 5.87 (s, CH<sub>2</sub>, 2H), 5.80 (s, CH<sub>2</sub>, 2H). <sup>13</sup>C NMR (DMSO-d<sub>6</sub>, 100.5 MHz, 25°C, δ, ppm): 162.8, 152.2, 144.6, 140.0, 139.5, 132.7, 131.3, 127.5, 126.6, 125.4, 124.4, 123.9, 121.6, 119.5, 114.7, 113.3, 112.5, 110.6, 109.7, 109.9, 108.6, 46.4, 45.6. Anal. Calcd for C<sub>32</sub>H<sub>25</sub>AgN<sub>4</sub> (%): C, 66.97; H, 4.36; N, 9.77; found (%): C, 66.69; H, 4.31; N, 9.62.

### 4.5 | Synthesis of complex 3

After adding the complex [Au(L)(Cl)] (90 mg, 0.17 mmol) to 10 ml of dichloromethane, an acetonitrile solution of [Ag(bpy)<sub>2</sub>]PF<sub>6</sub> (96 mg, 0.17 mmol) was introduced dropwise at room temperature; the formation of a white precipitate (AgCl) was immediately observed. After 2 h, the precipitate was removed through filtration, and then the solvent was evaporated. The residual solid was recrystallized from CH<sub>3</sub>CN-Et<sub>2</sub>O to afford the desired

complex as a colorless solid (96 mg, 0.12 mmol, 70% yield). Alternatively,  $[\text{Ag}(\text{L})(\text{bpy})]\text{[PF}_6]$  (90 mg, 0.17 mmol) was mixed with 15 ml of acetonitrile. Adding an acetonitrile solution of  $\text{Au}(\text{SMe}_2)\text{Cl}$  (90 mg, 0.17 mmol) dropwise resulted in the immediate precipitation of a white solid ( $\text{AgCl}$ ). Following a similar procedure to that described above afforded the desired complex in a comparable yield.  $^1\text{H}$  NMR ( $\text{DMSO}-d_6$ , 300 MHz, 25°C,  $\delta$ , ppm): 8.64 (d,  $J = 7.6$  Hz, bpy, 4H), 8.61 (m, bpy, 4H), 8.59 (d,  $J = 7.6$  Hz, py, 2H), 7.67 (m, py, 2H), 7.46 (d,  $J = 7.6$  Hz, bzimi, 2H), 7.44–7.41 (m, bzimi, 2H), 7.38 (d,  $J = 6.8$  Hz, bzyl, 2H), 7.31–7.28 (m, bzyl, 3H), 5.89 (s,  $\text{CH}_2$ , 2H), 5.83 (s,  $\text{CH}_2$ , 2H).  $^{13}\text{C}$  NMR ( $\text{DMSO}-d_6$ , 100.5 MHz, 25°C,  $\delta$ , ppm): 166.7, 154.5, 151.8, 149.5, 149.3, 148.9, 148.7, 148.4, 137.6, 137.5, 127.4, 126.3, 123.4, 122.3, 120.8, 118.0, 117.6, 116.5, 115.8, 114.6, 113.5, 112.6, 46.5, 45.8. Anal. Calcd for  $\text{C}_{30}\text{H}_{25}\text{N}_5\text{AuPF}_6$  (%): C, 45.17; H, 3.14; N, 8.78; found (%): C, 44.85; H, 3.10; N, 8.70.

## 4.6 | Synthesis of complex 4

A dichloromethane (50 ml) solution of complex  $[\text{Au}(\text{L})\text{Cl}]$  (191 mg, 0.38 mmol) was treated with carbazole (60 mg, 0.36 mmol) followed by NaOH (0.5 N, 2 ml) and  $\text{Bu}_4\text{NCl}$  (0.07 mmol). The resulting mixture was stirred for 2 days. Afterward, 50 ml of deionized water was added, and the resulting mixture was stirred for an additional hour. The organic component was extracted into dichloromethane and then concentrated to give a yellow residue. Recrystallization from  $\text{CH}_3\text{CN}$ - $\text{Et}_2\text{O}$  afforded the desired complex as a white solid (211 mg, 0.32 mmol, 85% yield).  $^1\text{H}$  NMR ( $\text{DMSO}-d_6$ , 300 MHz, 25°C,  $\delta$ , ppm): 8.58 (d,  $J = 7.6$  Hz, py, 2H), 8.03 (d,  $J = 4.8$  Hz, cbz, 2H), 7.79 (m, cbz, 4H), 7.67 (m, py, 2H), 7.50 (d,  $J = 5.8$  Hz, cbz, 2H), 7.46 (d,  $J = 7.6$  Hz, bzimi, 2H), 7.43–7.40 (m, bzimi, 2H), 7.38 (d,  $J = 6.8$  Hz, bzyl, 2H), 7.30–7.28 (m, bzyl, 3H), 5.89 (s,  $\text{CH}_2$ , 2H), 5.82 (s,  $\text{CH}_2$ , 2H).  $^{13}\text{C}$  NMR ( $\text{DMSO}-d_6$ , 100.5 MHz, 25°C,  $\delta$ , ppm): 164.4, 152.6, 144.8, 140.1, 139.7, 132.8, 131.4, 127.6, 126.8, 125.5, 124.6, 124.0, 121.7, 119.7, 114.8, 113.4, 112.7, 110.8, 109.8, 110.0, 108.7, 46.5, 45.8. Anal. Calcd for  $\text{C}_{32}\text{H}_{25}\text{AuN}_4$  (%): C, 58.01; H, 3.78; N, 8.46; found (%): C, 57.70; H, 3.74; N, 8.38.

## 4.7 | X-ray crystal structure determination

Single crystals suitable for X-ray data collection were grown by the slow diffusion of diethyl ether into a saturated acetonitrile solution of **1**, **2** or **4**. The crystal data and details of the data collections for the complexes are

given in Table 1. X-ray data were collected with a CCD diffractometer using graphite-monochromated Mo K $\alpha$  radiation (0.71073 Å). The structures were solved by direct methods and refined on  $F^2$  using all corrections using the SHELX-97 program.<sup>[25]</sup> The non-hydrogen atoms were anisotropically located. Hydrogen atoms that were not bound to imidazolium-C2 atoms were placed in calculated positions and assigned with an isotropic displacement parameter of 0.08.

## 4.8 | Computational methods

The complexes were fully optimized in the gas phase at the B3LYP-D3 level of theory<sup>[26]</sup> using the Gaussian 09 Revision D.01 quantum chemical program.<sup>[27]</sup> The silver and gold atoms were treated with the def2-TZVP basis set, which replaced the core 28 and 60 electrons, respectively, with an effective core potential and a triple-zeta valence basis set.<sup>[28]</sup> All other elements such as H, C and N were treated with the 6-31G\*\* basis set.<sup>[29]</sup> Hessian indices were used to elucidate the nature of the stationary states. NBO analyses were carried out on the optimized complexes using the B3LYP-D3/def2-TZVP (Ag, Au), 6-31G\*\* (C, H, N) level of theory.<sup>[30]</sup>

## SUPPORTING INFORMATION AVAILABLE

Crystallographic data for complexes **1**, **2** and **4** are available free of charge at <http://www.ccdc.cam.ac.uk>.

## NOTES

The authors declare no competing financial interest.

## ACKNOWLEDGMENTS

J.D. is grateful to the DST, Government of India for financial support through project EMR/2016/007022. C.W.B. acknowledges the Institute for Basic Science (grant IBS-R019) as well as the BK21 Plus Program as funded by the Ministry of Education and the National Research Foundation of Korea for support. J.D. is grateful to Mr. P. Mitra for solid-state structural studies.

## ORCID

Christopher W. Bielawski  <https://orcid.org/0000-0002-0520-1982>

Joydev Dinda  <https://orcid.org/0000-0002-8780-6300>

## REFERENCES

- [1] A. J. Arduengo, R. L. Harlow, M. Kline, *J. Am. Chem. Soc.* **1991**, *113*, 361.

- [2] (a) D. Bourissou, O. Guerret, F. P. Gabbai, G. Bertrand, *Chem. Rev.* **2000**, *100*, 39. (b) K. Öfele, *J. Organometal. Chem.* **1968**, *12*, 42. (c) H. W. Wanzlick, H. J. Schonherr, *Angew. Chem. Int. Ed.* **1968**, *7*, 141.
- [3] (a) P. de Fremont, N. Marion, S. P. Nolan, *Coord. Chem. Rev.* **2009**, *253*, 862. (b) W. A. Herrmann, C. Kocher, *Angew. Chem. Int. Ed.* **1997**, *36*, 2162.
- [4] O. Schuster, L. Yang, H. G. Raubenheimer, M. Albrecht, *Chem. Rev.* **2009**, *109*, 3445.
- [5] (a) J. C. Garrison, W. J. Youngs, *Chem. Rev.* **2005**, *105*, 3978. (b) A. K. Nebioglu, M. J. Panzner, C. A. Tessier, C. L. Cannon, W. J. Youngs, *Coord. Chem. Rev.* **2007**, *251*, 884. (c) W. Liu, R. Gust, *Chem. Soc. Rev.* **2013**, *42*, 755. (d) G. Roymahapatra, S. M. Mandal, W. F. Porto, T. Samanta, S. Giri, J. Dinda, O. L. Franco, P. K. Chattaraj, *Curr. Med. Chem.* **2012**, *19*, 4184. (e) T. Samanta, G. Roymahapatra, W. F. Porto, S. Seth, S. Ghorai, S. Saha, J. Sengupta, O. L. Franco, J. Dinda, S. M. Mandal, *PLoS ONE* **2013**, *8*, e58346.
- [6] (a) D. T. Weiss, S. Haslinger, C. Jandl, A. Pöthig, M. Cokoja, F. E. Kühn, *Inorg. Chem.* **2015**, *54*, 415. (b) A. Vellé, A. Cebollada, M. Iglesias, P. J. S. Miguel, *Inorg. Chem.* **2014**, *53*, 10654.
- [7] C. Mejuto, G. G. Barrios, D. Gusev, E. Peris, *Chem. Commun.* **2015**, *51*, 13914.
- [8] (a) V. W. W. Yam, V. K. M. Au, S. Y. L. Leung, *Chem. Rev.* **2015**, *115*, 7589. (b) J. C. Y. Lin, R. T. W. Huang, C. S. Lee, A. Bhattacharyya, W. S. Hwang, I. J. B. Lin, *Chem. Rev.* **2009**, *109*, 3561.
- [9] (a) V. J. Catalano, M. A. Malwitz, *Inorg. Chem.* **2003**, *42*, 5483.
- [10] (a) L. Benhamou, E. Chardon, G. Lavigne, S. B. Laponnaz, V. Cesar, *Chem. Rev.* **2011**, *111*, 2705. (b) B. M. Neilson, C. W. Bielawski, *J. Am. Chem. Soc.* **2012**, *134*. (c) D. Pugh, A. A. Danopoulos, *Coord. Chem. Rev.* **2007**, *251*, 610.
- [11] E. C. Constable, *Adv. Inorg. Chem.* **1986**, *30*, 69.
- [12] F. Cui, P. Yang, X. Huang, X. J. Yang, B. Wu, *Organometallics* **2012**, *31*, 3512.
- [13] M. H. Reineke, T. M. Porter, A. L. Ostericher, C. P. Kubiak, *Organometallics* **2018**, *37*, 448.
- [14] H. M. J. Wang, C. S. Vasam, T. Y. R. Tsai, S. H. Chen, A. H. H. Chang, I. J. B. Lin, *Organometallics* **2005**, *24*, 486. and references therein
- [15] S. D. Adhikary, L. Jhulki, S. Seth, A. Kundu, V. Bertolasi, P. Mitra, A. Mahapatra, J. Dinda, *Inorg. Chim. Acta* **2012**, *384*, 239.
- [16] M. C. Jahnke, T. Pape, F. E. Hahn, *Eur. J. Inorg. Chem.* **2009**, *13*, 1960.
- [17] X. Zhang, S. Gu, Q. Xia, W. Chen, *J. Organometal. Chem.* **2009**, *694*, 2359.
- [18] H. M. J. Wang, C. Y. L. Chen, I. J. B. Lin, *Organometallics* **1999**, *18*, 1216.
- [19] L. Jhulki, P. Dutta, M. K. Santra, M. H. Cardoso, K. G. N. Oshiro, O. L. Franco, V. Bertolasi, A. A. Isab, C. W. Bielawski, J. Dinda, *New J. Chem.* **2018**, *42*, 13948.
- [20] R. Santra, K. Banerjee, K. Biradha, *Chem. Commun.* **2011**, *47*, 10740.
- [21] (a) S. S. Batsanov, *Inorg. Materials* **2001**, *37*, 871. (b) A. J. Martinez, *Braz. Chem. Soc.* **2005**, *16*, 337.
- [22] D. Pathak, S. Deuri, P. Phukan, *J. Phys. Chem. A* **2016**, *120*, 128.
- [23] V. Rani, H. B. Singh, R. J. Butcher, *Organometallics* **2017**, *36*, 4741.
- [24] T. P. Pell, D. J. D. Wilson, B. W. Skelton, J. L. Dutton, P. J. Barnard, *Inorg. Chem.* **2016**, *55*, 6882.
- [25] G. M. Sheldrick, *SHELX97, Program for Crystal Structure Refinement*, University of Gottingen, Germany **1997**.
- [26] S. Grimme, J. Antony, S. Ehrlich, H. A. Krieg, *J. Chem. Phys.* **2010**, *132*, 154104.
- [27] M. J. Frisch, G. W. Trucks, H. B. Schlegel, G. E. Scuseria, M. A. Robb, J. R. Cheeseman, J. A. Montgomery Jr., T. Vreven, K.N. Kudin, J.C. Burant, J. M. Millam, S. S. Iyengar, J. Tomasi, V. Barone, B. Mennucci, M. Cossi, G. Scalmani, N. Rega, G. A. Petersson, H. Nakatsuji, M. Hada, M. Ehara, K. Toyota, R. Fukuda, J. Hasegawa, M. Ishida, T. Nakajima, Y. Honda, O. Kitao, H. Nakai, M. Klene, X. Li, J. E. Knox, H. P. Hratchian, J. B. Cross, V. Bakken, C. Adamo, J. Jaramillo, R. Gomperts, R. E. Stratmann, O. Yazyev, A. J. Austin, R. Cammi, C. Pomelli, J. W. Ochterski, P. Y. Ayala, K. Morokuma, G. A. Voth, P. Salvador, J. J. Dannenberg, V. G. Zakrzewski, S. Dapprich, A. D. Daniels, M. C. Strain, O. Farkas, D. K. Malick, A. D. Rabuck, K. Raghavachari, J. B. Foresman, J. V. Ortiz, Q. Cui, A. G. Baboul, S. Clifford, J. Cioslowski, B. B. Stefanov, G. Liu, A. Liashenko, P. Piskorz, I. Komaromi, R. L. Martin, D. J. Fox, T. Keith, M. A. Al-Laham, C. Y. Peng, A. Nanayakkara, M. Challacombe, P. M. W. Gill, B. Johnson, W. Chen, M. W. Wong, C. Gonzalez and J. A. Pople, Gaussian 03, Revision D.01, Gaussian Inc., Wallingford, CT, 2004.
- [28] (a) F. Weigend, R. Ahlrichs, *Phys. Chem. Chem. Phys.* **2005**, *7*, 3297. (b) F. Weigend, *Phys. Chem. Chem. Phys.* **2006**, *8*, 1057.
- [29] (a) W. J. Hehre, R. Ditchfield, J. A. Pople, *J. Chem. Phys.* **1972**, *56*, 2257. (b) P. C. Hariharan, J. A. Pople, *Theor. Chim. Acta* **1973**, *28*, 213.
- [30] (a) A. E. Reed, L. A. Curtiss, F. Weinhold, *Chem. Rev.* **1988**, *88*, 899. (b) E. D. Glendening, A. E. Reed, J. E. Carpenter, F. Weinhold, *NBO Version 3.1*, Gaussian Inc., Wallingford, CT **2009**.

**How to cite this article:** Das Adhikary S, Mondal A, Kisan HK, Bielawski CW, Dinda J. Bipyridyl/carbazolate silver(I) and gold(I) N-heterocyclic carbene complexes: A systematic study of geometric constraints and electronic properties. *Appl Organometal Chem.* 2019;e5335. <https://doi.org/10.1002/aoc.5335>